microplastics

MDPI

Article

From Microplastics to "Mycoplastics": Enzymatic Conversion of Oxidized Polystyrene into Humic Acid-like Products

Filippo Petri [1], Daria Armani [1,2], Andrea Corti [1,3], Michele Lancia [4,5], Antonella Petri [1,*] and Valter Castelvetro [1,3,*]

[1] Department of Chemistry and Industrial Chemistry, University of Pisa, 56124 Pisa, Italy; filippo.petri12@gmail.com (F.P.); daria.armani2@unibo.it (D.A.); andrea.corti@unipi.it (A.C.)
[2] Department of Industrial Chemistry "Toso Montanari", University of Bologna, 40129 Bologna, Italy
[3] CISUP—Center for the Integration of Scientific Instruments of the University of Pisa, University of Pisa, 56127 Pisa, Italy
[4] Eastern Institute for Advanced Studies, Eastern Institute of Technology, Ningbo 315200, China; lancia@eitech.edu.cn
[5] State Environmental Protection Key Laboratory of Integrated Surface Water-Groundwater Pollution Control, School of Environmental Science and Engineering, Southern University of Science and Technology, Shenzhen 518055, China
* Correspondence: antonella.petri@unipi.it (A.P.); valter.castelvetro@unipi.it (V.C.)

Abstract

The environmental degradation of plastics results not only in their mechanical fragmentation into microplastics (MPs), but also in polymer main-chain scission processes, causing continuous leaching and/or volatilization of low-molecular-weight species, often characterized by a hazardous profile. In this study, we investigated the hydrophilic photooxidation products (HyPOPs) generated upon UV irradiation of polystyrene (PS) and their transformation catalyzed by the enzyme laccase from the fungus *Trametes versicolor*. Through a series of enzymatic tests, the enzyme was found to promote coupling and conjugation reactions of HyPOPs into poorly soluble compounds mimicking natural humic acids. The enzymatic activity of laccase was studied under different experimental conditions to simulate those found in environmental matrices. Due to their oligomeric nature, these humic acid-like products of metabolic transformation by the fungal laccase are here nicknamed "mycoplastics" (i.e., polymers from fungi). This enzymatic biodegradation and biotransformation of xenobiotic HyPOPs highlights the role of specific enzymes as biological tools for environmental self-repair of polluted ecosystems. Moreover, it opens new perspectives for remediation strategies targeting elusive micro- and nanoplastics and their continuously generated hazardous molecular degradation by-products. Humic acid-like products resulting from laccase conversion of HyPOPs could contribute to the rehabilitation of contaminated sites by promoting the removal of toxic contaminants from soil and water.

Keywords: polystyrene microplastics; photodegradation products; laccase; enzymatic oxidation; enzymatic oligomerization

Check for updates

Academic Editor: Nicolas Kalogerakis

Received: 17 December 2025
Revised: 20 January 2026
Accepted: 5 February 2026
Published: 2 March 2026

Copyright: © 2026 by the authors. Licensee MDPI, Basel, Switzerland. This article is an open access article distributed under the terms and conditions of the Creative Commons Attribution (CC BY) license.

1. Introduction

Polystyrene (PS), one of the most widely used plastic commodities together with polyethylene (PE), polypropylene (PP) and polyethylene terephthalate (PET), has revolutionized modern industry thanks to its versatility, light weight, and low cost [1]. The polymeric materials mentioned above, characterized by their ability to maintain their

properties over long service lifetime, are nevertheless mostly employed to produce disposable single-use items. Recycling these materials is often not cost-effective, and their ever-increasing production, diffuse utilization and frequent end-of-life mismanagement are leading to growing environmental pressure from plastic waste, while also raising concerns about potential impacts on human health [2]. Over the last decade, an increasing number of studies have investigated the fate of plastic waste dispersed in the environment, resulting in the progressive fragmentation of macroscopic objects or debris into increasingly smaller particles. Such particles, also known as microplastics (MPs, often referred to as particles between 5 mm and 1 µm) and nanoplastics (NPs, particles smaller than 1 µm), can infiltrate a wide range of terrestrial and aquatic ecosystems and exhibit enhanced toxicity [3]. Ingestion of MPs by marine organisms has been linked to damage to the gastrointestinal and vascular systems, adversely affecting survival and reproduction. Similarly, the accumulation of MPs and NPs (hereafter collectively referred to as MNPs) in agricultural soil raises concerns about food safety due to the transfer of such hazardous materials into the food chain [4]. Most studies on the adverse health effects of MNPs are based on commercially available PS micro- and nanospheres as model environmental MNPs [5]. Despite the relative chemical inertness of these model MNPs compared to real environmentally degraded ones, PS MNPs have been reported as suspected carcinogenic and neurotoxic materials, with potential adverse effects on the reproductive system [6]. Styrene, found in human skin and breast milk samples—likely due to a combination of various possible sources, including degradation products of PS MNPs—has been linked to chromosomal damage, abnormal pulmonary function, and cancer in workers exposed to styrene vapors [7–9].

In this scenario, it is essential to understand the ultimate environmental fate of PS by-products deriving from weathering processes. Indeed, fragmentation of PS as a result of photooxidative degradation increases the available surface area and the surface oxidation level, thereby enhancing the potential for microbial decomposition. This process represents a possible bioremediation pathway for PS MPs in soil and similar environmental matrices [10–14]. However, environmental degradation of PS also results in the generation and release of molecular and oligomeric fragments, typically hydrophilic photooxidation products (HyPOPs) [15,16]. While it is important to identify the chemical transformation pathways from PS down to HyPOPs, another less investigated but possibly highly relevant issue concerns the pathways and products of their subsequent enzymatic conversion [17]. In fact, while photooxidative degradation of PS may be beneficial for the self-remediation of polluted soils, several of the HyPOPs generated during these processes may also be harmful or even more toxic than the parent material [16,18].

Photooxidative degradation of PS is known to result in a range of phenolic derivatives, including those bearing carbonyl and carboxyl moieties. For example, catechol (C), salicylic acid (o-hydroxybenzoic acid, o-OH-BA) and p-hydroxybenzoic acid (p-OH-BA) are typically among the most abundant HyPOPs generated upon photochemical degradation of PS [19]. Catechol is associated with skin irritation and acute eczema and is a suspected human carcinogen [20,21]. Benzoic acid, commonly used as an antimicrobial agent in food products, may induce anaphylactic shock in sensitive individuals, while its hydroxylated analog o-OH-BA may cause hypoglycemia, laryngopharyngeal irritation, and nausea. In contrast, p-OH-BA has no major health effects at low concentrations but may cause irritation of the respiratory tract and possible liver or blood toxicity at higher concentrations [22,23]. Therefore, the bioconversion of these compounds into less toxic chemicals would be a potentially impactful environmental (self-)remediation mechanism.

Several enzymes have been identified as being involved in the environmental degradation of fossil-based polymers [24]. Among them, laccases, a family of copper-containing oxidoreductase enzymes produced by many microorganisms, plants, and fungi [25,26],

play an important role in the biodegradation of the semi-aromatic biopolymer family of lignins. It is also well known that phenolic substrates can be converted into more highly oxidized products and high-molecular-weight oligomeric compounds through coupling and polymerization reactions catalyzed by laccase [27]. These oxidoreductases catalyze single-electron transfer (SET) reactions for a wide variety of substrates through the formation of phenoxy radicals coupled with the reduction of molecular oxygen [28]. The activity of laccase may thus contribute to soil detoxification through the biosynthetic conversion of noxious HyPOPs into new compounds with bioremediation and bioaugmentation potential [29]. Indeed, several phenolic derivatives can be transformed by laccase into their high-molecular-weight analogs via the formation of aromatic and quinone radical intermediates followed by rearrangement and ring closure steps [30–32]. In particular, laccase can promote the conversion of chalcone-like compounds into oligomeric species with humic acid-like structures [31]. Similar mechanisms are involved in the biosynthetic routes to lignin through polymerization of natural hydroxyphenyl propenols by various oxidative enzymes.

Additional attractive features of laccases include their high specificity and activity under mild pH and temperature conditions, as well as their participation in reactions with a net reduction in the environmental burden, since they use molecular oxygen as an electron acceptor, generating water as the sole by-product [33,34]. All the above features make these oxidoreductases very promising candidates for investigating the transformation and fate of oxidized aromatic compounds resulting from the photochemical degradation of PS MPs under environmental conditions.

In this work, the activity of the laccase from *Trametes versicolor* was investigated to assess its activity toward HyPOPs generated upon the photooxidative degradation of artificially aged PS MPs, with particular emphasis on the biotransformation of such HyPOPs into humic acid-like species. Humic acids are known to improve agricultural soil fertility by retaining organic matter and essential mineral nutrients [35]. Therefore, the potential bioconversion of HyPOPs from aqueous leachates of photooxidized PS into less hazardous molecular species—and, in particular, into higher-molecular-weight humic acid-like products—may represent an important route for environmental self-remediation.

Among the challenges to be considered, the low concentrations of HyPOPs and the possible inhibition of the enzymatic activity by the broad spectrum of molecular and oligomeric compounds resulting from the oxidative degradation of PS [27] account for the complexity of such an investigation.

2. Materials and Methods

2.1. Chemicals

The HPLC-grade solvents methanol, acetonitrile (MeCN), trifluoroacetic acid (TFA), water, p-hydroxy-acetophenone (p-OH-AP), acetophenone (AP) and laccase from *Trametes versicolor* (0.9 U/mg) were purchased from Merck (Sigma Aldrich, St. Louis, MO, USA). Catechol (C) was purchased from Tokyo Chemical Industry (TCI Europe N.V., Paris, France). Benzoic acid (BA), p-hydroxy-benzoic acid (p-OH-BA) and syringaldazine were purchased from Carlo Erba Reagents (Milan, Italy). Unless otherwise specified, all solvents and chemicals were used without any further purification. Polystyrene Crystal25 (nominal density 1.05 g/cm^3, average particle size 564 μm) micronized powder produced by cryogenic quenching from the melt was a kind gift from Poliplast S.p.A. (Casnigo, Italy).

2.2. Equipment and Techniques

A Bruker (Bruker Italia Srl, Milan, Italy) IFS 66 FT-IR spectrometer was used to follow the progress of PS photooxidation. Transmission mode spectra were recorded in the

4000–400 cm^{-1} range at 4 cm^{-1} resolution from samples pressed in a KBr pellet. A total of 32 transients were collected before the FT calculations.

Gel permeation chromatography (GPC) analyses were performed on a Jasco (Jasco Europe Srl, Cremella, Italy) liquid chromatography apparatus consisting of a PU-2089Plus pump, a column oven set at 30 °C and a PI-2031 refractive index detector. Next, 100 µL of a 0.5% *w*/*v* sample solution in $CHCl_3$ was eluted with $CHCl_3$ at a 1 mL min^{-1} flow rate. Number-average molecular weight ($\overline{M}_n$), weight-average molecular weight ($\overline{M}_w$) and polydispersity index (PI) were calculated from a polystyrene standard calibration curve (range 0.5–300 kDa). Two PL gel 5 µm Mixed-D columns were used for the analysis of PS, while low-molecular-weight fractions (e.g., methanol extracts from degraded PS) were analyzed under the same conditions by using a Phenogel (Phenomenex srl, Castel Maggiore, Italy) TM 5 µm 500 Å LC Column 300 mm length × 7.8 mm diameter and a Phenogel TM 5 µm 100 Å LC Column 300 mm length × 7.8 mm diameter connected in series.

Gas chromatography–mass spectroscopy (GC-MS) analyses of MeCN extracts were carried out on a mod. 7890B Agilent gas chromatograph (Agilent Technologies Italia S.p.A., Cernusco sul Naviglio, Italy) equipped with an MMI inlet, a mod. 7693A automatic liquid sampler, and a mod. 7010 triple-quadrupole mass spectrometer, along with the dedicated software and GC/MS-MS spectral library for qualitative and quantitative analysis.

UPLC-MS analyses of methanol extracts were performed on a Waters (Waters SpA, Sesto San Giovanni, Italy) Acquity UPLC instrument coupled with a Waters Acquity QDa mass spectrometer, with the probe set to 600 °C, ESI capillary voltage to 1.5 V, cone voltage to 15 V, and mass range to 60–1000, equipped with an Acquity UPLC BEH C18 1.7 µm, 75 mm length × 2.1 mm diameter column. Gradient elution was performed by combining Phase A (95/5 H_2O/MeCN + 0.1% formic acid) and Phase B (5/95 H_2O/MeCN + 0.1% formic acid) at a 0.6 mL/min flow rate.

HPLC analyses, performed for the identification and quantification of compounds based on calibration lines built by using reference test substrates, were carried out on a Jasco HPLC system consisting of a PU-2089 Plus pump, AS-2057 Plus autosampler, CO-2060 Plus column oven, MD910 Diode Array UV Detector (HPLC-DAD) and Phenomenex-Aqua C18 column (250 mm × 4.6 mm, 5 µm particle size). Standard solutions prepared from a 1 mg/mL aqueous stock solution of C, p-OH-AP and p-OH-BA, diluted with a 1:1 H_2O:MeCN mixture, were used to build the calibration curves. Elution was performed with 90:10:0.1 H_2O:MeCN:TFA (r.t. 6.14 min, 13.38 min, and 7.27 min for C, p-OH-AP and p-OH-BA, respectively). The linear fit parameters of the calibration (y = ax + b mg/mL) were a = 244.3 and b = 3.765 for C (R^2 = 0.9973, LOD= 0.0002, LOQ= 0.0009), a = 147.3 and b = 0.5188 for p-OH-AP (R^2 = 0.9996, LOD = 0.001, LOQ = 0.004), a = 249.15 and b = 2.083 for BA (R^2 = 0.9998, LOD= 0.003, LOQ= 0.010), and a = 251.6 and b = 1.919 for p-OH-BA (R^2 = 0.9995, LOD= 0.001, LOQ= 0.004) (Figures S1–S4 and Tables S1 and S2 in the Supplementary Information, SI).

UV–Vis spectrophotometric analyses were carried out with a Shimadzu (Shimadzu Italia srl, Milan, Italy) UV-2600i spectrophotometer. ^1H NMR spectra were recorded with a Jeol ECZR 400 MHz and a Jeol ECZR 500 MHz (Jeol Italia SpA, Basiglio, Italy) spectrometer. Chemical shifts are reported in ppm and refer to the signal of the residual ^1H in the deuterated $CDCl_3$ used as the solvent.

2.3. UV Degradation Tests

Photo-aging of the PS micropowder was performed with a Polymer 400 W medium-pressure mercury UV lamp (Helios Italquartz srl, Cambiago, Italy) at irradiation intensities of Ee254 = 13.4 W/cm^2 and Ee365 = 18.4 W/cm^2 at 254 and 365 nm, respectively, as measured with a radiometer at 15 cm distance from the lamp. Photooxidation under dry

conditions was performed by 2–5 h irradiation on 5 g of PS micropowder evenly distributed (about 0.15 cm thickness) in a Petri dish and manually stirred at 1 h intervals (PS_d-UV). At the end of the treatment, the PS micropowder was stored in a closed flask flushed with nitrogen. Photooxidation in deionized water was performed on PS micropowder suspensions (5 g PS in 30 mL of water) loaded in closed quartz test tubes and kept under magnetic stirring (75 rpm) up to 5 h irradiation (PS_w-UV). At the end of the irradiation, each aqueous PS suspension was filtered through a 0.2 µm PVDF filter and the aqueous phase was concentrated to a small volume at reduced pressure prior to analytical characterization and enzymatic testing.

2.4. Extraction Procedures of PS and Relevant Photodegradation Products

2.4.1. Pristine PS Purification from Water-Soluble Products and Additives

In order to remove any water-soluble products and additives present in pristine PS micro powder, 20 g of PS were placed in a cellulose thimble and extracted for 5 h with H_2O at reflux using a Kumagawa apparatus. Once the indicated time had elapsed, the PS in the thimble was dried and used in the photochemical oxidation tests.

2.4.2. Extraction of UV-Irradiated PS with Water

To collect water-soluble products produced during the UV irradiation, 2.5 g of PS_d-UV aged 5 h (PS_d-UV-5h) and 30 mL of deionized H_2O were introduced in a 100 mL Erlenmeyer flask, and the mixture was stirred for 24 h at room temperature. The mixture was then filtered through a 0.22 µm PVDF filter, dried to constant weight and then submitted for analytical characterizations.

2.4.3. Extraction of UV-Irradiated PS with Methanol

To collect medium- and low-molecular-weight degradation products, 2.5 g of PS_d-UV-5h and 30 mL MeOH were introduced in a 100 mL Erlenmeyer flask, and the mixture was kept stirring for 24 h. The procedure was repeated two times. Subsequently, the two organic solvent fractions were combined and filtered through a 0.22 µm PVDF filter, dried to constant weight, and then subjected to analytical characterizations.

2.4.4. Extraction of Aqueous Phase from PS Irradiation in Water

To extract water-soluble by-products from the PS degradation tests, the aqueous phase was added with an equal volume of MeCN and left to cool at −20 °C. The organic solvent was separated from the frozen aqueous phase and the procedure was repeated twice. The combined organic phases were dried to constant weight and analyzed with GC-MS.

2.5. Enzymatic Reactions

Unless otherwise specified, enzymatic tests were carried out in 2.0 mL Eppendorf safe-lock tubes incubated in an Eppendorf Thermomixer (Eppendorf srl, Milan, Italy) at 30 °C and 600 rpm. In parallel, enzyme-free reactions were carried out as reference blank tests. Tests were carried out, unless otherwise specified, using a substrate/laccase 1:2 weight ratio up to 96 h of incubation, monitoring the conversion every 24 h. The reactions were performed in distilled water and for comparison in citrate buffer (100 mM, pH = 5); in both cases, experiments were performed with and without the addition of 10 vol% methanol.

2.6. Laccase Activity Assays

The spectrophotometric activity assays for laccase were performed by following an already reported procedure [36]. Two quartz cuvettes were loaded with 2.2 mL buffer + 0.5 mL water or 0.5 mL of enzymatic solution, respectively (blank solutions to set the zero-absorbance background), followed by addition of 0.3 mL of a 0.216 mM syringaldazine

solution in MeOH to each cuvette and shaking before acquisition of the UV spectra. The increase in absorbance at 530 nm upon oxidation of phenolic groups of syringaldazine (upon this conversion the solution turned from yellow to pink) was monitored for 3 min after syringaldazine addition. The number of enzymatic activity units was calculated from the slope of the linear fit d(Abs)/d(t).

3. Results and Discussion

To investigate the possible role played by enzymes in the environmental fate of synthetic polymer micropollutants, we selected a micropowder of photooxidized PS and laccase, a fungal enzyme involved in lignin biochemistry, as a model system representative of a soil contaminated by PS MNPs. We were particularly interested in assessing the effectiveness of laccase in the conversion of the low-molecular-weight degradation products generated upon photooxidative aging of PS. Such degradation products are generated and continuously released as the end products of complex degradation pathways activated by the exposure to solar irradiation and largely involving free-radical processes. The latter are associated with atmospheric oxygen uptake and the consequent generation of oxidized moieties, also involving C-C bond cleavage, eventually leading to the release of low-molecular-weight molecules [37].

3.1. Degradation Products of PS upon UV Irradiation

A virgin PS micropowder, produced by cryomilling and purified by continuous extraction with hot water, was subjected to accelerated photooxidative aging under UV irradiation to simulate the product of PS environmental aging and thus obtain microplastic particles along with low-molecular-weight PS degradation products. Such molecules, deriving from photo-aged PS, were then thoroughly analyzed to identify and select the target substrates to be tested in the subsequent enzymatic degradation experiments.

UV irradiation was performed under both dry (PS_d-UV) and wet (PS_w-UV) conditions, representative of two common environmental exposure routes, such as dispersion on sandy beaches or agricultural soil and floatation in surface waters.

UV irradiation of 5 g PS either in 30 mL of deionized H_2O or as a thin layer of dry powder caused rapid yellowing, indicative of the generation of conjugated chromophoric structures as confirmed by the FTIR spectra of PS_w-UV (Figure 1). This process was faster under wet conditions, with yellowing already noticed after 1 h of irradiation as compared to 5 h irradiation under dry conditions.

The presence of oxidized groups in PS_w-UV-5h (PS_w after 5 h of UV irradiation) is clearly shown by the occurrence, in its FT-IR spectrum, of a broad OH stretching absorption centered at about 3400 cm^{-1}, the C=O absorption between 1730 and 1700 cm^{-1}, the shoulder of the aromatic ring stretching band (peaking at 1600 cm^{-1}) around 1680 cm^{-1}, and the various C-O stretching bands from oxidized alkyl and alkylaromatic moieties at 1200 cm^{-1} and 1310 cm^{-1}. Similar absorption bands from functional groups were also detected in the case of PS_d-UV after 5h of UV irradiation.

GPC analysis of polymer residues and methanol-extractable fractions obtained from PS samples after 2 and 5 h of irradiation confirmed the photooxidative degradation of PS involving backbone main-chain scission processes. In detail, GPC analysis carried out on dried methanol extracts of PS_d-UV-2h gave $\overline{M}_n$ values around 380 Da, roughly corresponding to a styrene tetramer. In addition, a slight but progressive decrease over time (PS_d-UV-5h) in both the number-average molecular weight ($\overline{M}_n$) and the weight-average molecular weight ($\overline{M}_w$) was observed (Table 1), along with an increase in the polydispersity index (PDI = $\overline{M}_w/\overline{M}_n$).

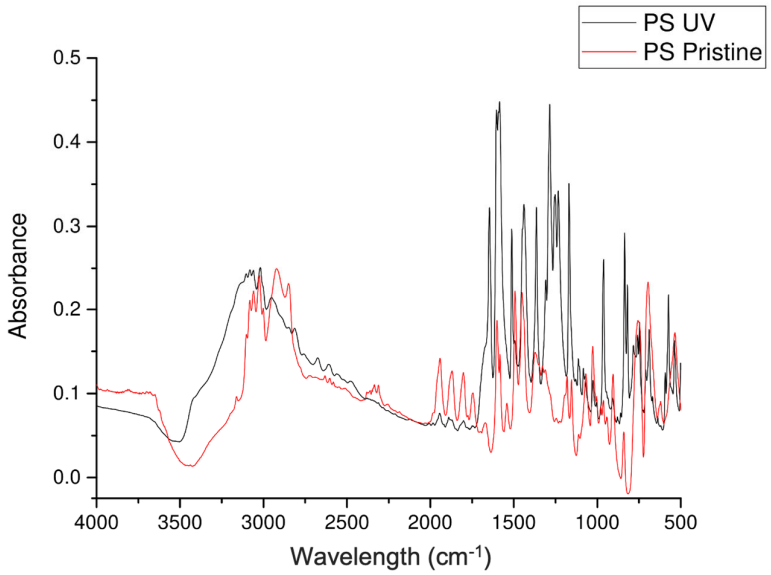


Figure 1. FTIR spectra of pristine (red line) and aged (PS_w-UV-5h, black line) PS: 3400 cm^{-1} OH stretching; 1730, 1700 cm^{-1} C=O stretching; 1680 cm^{-1} aromatic ring stretching.

Table 1. GPC data for PS_d-UV after irradiation.

Sample	Polymer Residue			Methanol Extractables		
	$\bar{M}_n$ [kDa]	$\bar{M}_w$ [kDa]	PDI	$\bar{M}_n$ [kDa]	$\bar{M}_w$ [kDa]	PDI
PS	54.873	110.392	2.001	-	-	-
PS_d-UV-2h	48.913	108.270	2.213	0.377	0.652	1.60
PS_d-UV-5h	46.769	105.338	2.257	0.399	0.670	1.62

The increase in PDI indicates main-chain scission reactions initially and preferentially occurring within the outer surface layer of the particle due to diffusion-limited reactivity of newly generated carbon radicals with molecular oxygen. The resulting peroxy radicals, most likely phenyl-substituted tertiary carbons, are known to initiate a cascade amplification of free-radical-generating reactions typically involving, as a first step, the formation of thermally and photochemically unstable hydroperoxides. These easily decompose by homolytic peroxide cleavage, generating two new radicals (cascade amplification of free-radical species), namely a highly reactive and mobile hydroxyl radical and an alkoxy macroradical. The latter may transfer the radical by abstracting a hydrogen atom from a nearby polymer chain and turn into a main-chain alcohol or undergo β-scission of either the C-phenyl bond or the C-CH_2 bond [37–40].

C-phenyl cleavage leads to a main-chain ketone and a highly reactive phenyl radical, whereas main-chain C-CH_2 cleavage generates a terminal macroradical that can further react by oxygen addition, isomerization to generate a relatively more stable tertiary radical, or Norrish type I reactions yielding terminal ketones and acetophenone, which can eventually further oxidize to form carboxylic acid derivatives [37–40].

The ensuing reduction in average polymer chain length would result in a decrease in PDI if the process were uniform throughout the material; in contrast, it would lead to an increase in PDI if the process did not proceed with the same rate throughout the material, due to slower polymer photooxidation in the particle core because of the diffusion-limited concentration of oxygen. The occurrence of extensive chain scission involving at least a fraction of the photo-aged PS micropowder was confirmed by the higher PDI and the presence of methanol-extractable low oligomers (Table 1).

While FTIR and GPC results gave semi-quantitative information on the extent of oxidation and fragmentation of the macromolecular chain averaged over the entire photo-aged sample, details on the species generated by the chain scission reactions were obtained by GC-MS and UPLC-MS-DAD chromatographic analyses.

First, PS_d-UV-5h was extracted at room temperature with H_2O and analyzed by GC-MS (Table S3 in the SI). Among the detected aromatic and aliphatic species, the most abundant were 3-ethylbenzoic acid, 4-hydroxy-3-methoxybenzaldehyde and acetophenone, all well-known photochemical degradation products of PS [41–43].

Low-molecular-weight water-soluble degradation products are of environmental significance because they are more readily bioavailable. Their leaching from the photo-aged PS MPs is facilitated by extensive surface oxidation, with the resulting polar groups make the outer particle layer more hydrophilic and thus less impervious to water penetration, thereby enhancing the extraction efficiency for water-soluble molecular or oligomeric PS degradation products [44].

PS_d-UV-5h was also extracted with MeOH (PS_d-UV-MeOH) and the extract was analyzed by UPLC-MS-DAD (see following Section 3.2.3) and HPLC-DAD, complementing the information from the previous experiment on the more polar and lower- molecular-weight products leached into water.

UPLC-MS-DAD analysis revealed the presence of p-hydroxybenzoic acid (p-OH-BA), benzoic acid (BA), p-hydroxyacetophenone (p-OH-AP), catechol (C), acetophenone (AP), and salicylic acid as well as other dozens of unidentified products in the 100–1000 m/Z range with different polarity, as indicated by their detection over a broad range of retention times. The HPLC-DAD results (Figure 2) confirmed the presence of the most abundant compounds already detected by UPLC-MS-DAD in the methanol extract, along with several unidentified high-molecular-weight compounds [19].

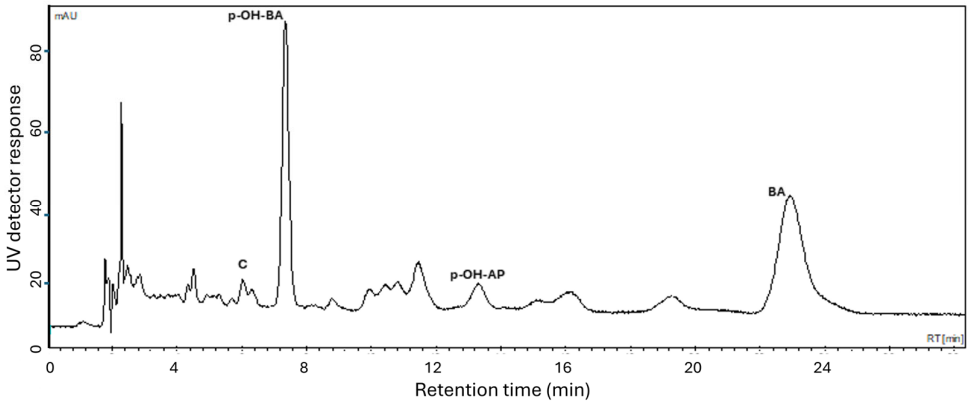


Figure 2. HPLC-DAD chromatogram (254 nm) of the methanol extract PS_d-UV-MeOH.

It should be noted that the UV irradiation at 254 nm used in this work to promote faster degradation of PS may activate some reaction pathways less likely to occur under environmental conditions. However, while the degradation kinetics and pathways may not exactly mirror those occurring in the environment, the main products identified in the MeOH extracts have also been reported or hypothesized in other studies in which photo-aging was performed using fluorescent xenon lamps that more closely match the solar spectrum [45].

Furthermore, the same compounds C, p-OH-BA, p-OH-AP and BA were also directly detected in the aqueous phase obtained from the irradiation of PS under wet conditions. HPLC-DAD analysis (Figure 3) substantially confirmed that water plays a negligible role in the degradation mechanism [46,47].

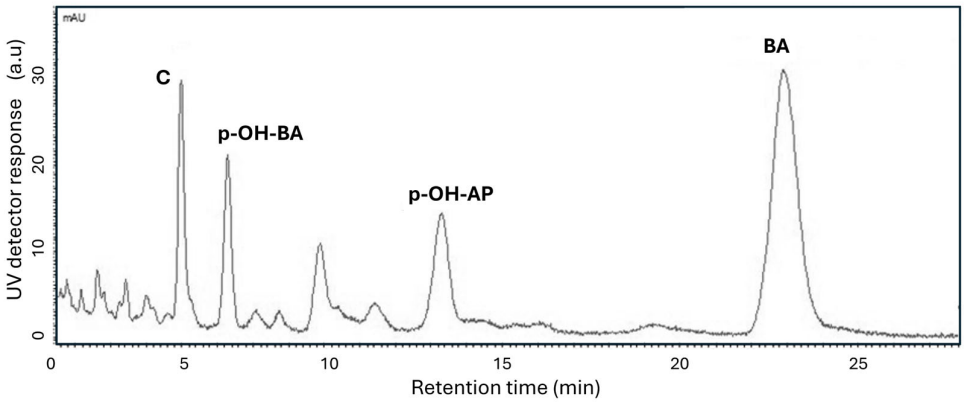


Figure 3. HPLC-DAD chromatogram (254 nm) of the aqueous phase obtained after irradiation of PS under wet conditions.

3.2. Enzymatic Tests

The most abundant identified products of PS photooxidation, namely p-OH-BA, BA, p-OH-AP, and C, were used as substrates for potential enzymatic conversion by *Trametes versicolor* laccase. The catalytic performance of the enzyme was first tested in the biotransformation of the corresponding commercial individual compounds and their simple mixture to assess the optimal reaction conditions. Subsequently, laccase conversion was studied on PS_d-UV extracts. Unless otherwise specified, a substrate/laccase weight ratio of 1:2 was used.

3.2.1. Enzymatic Reactions on C, p-OH-AP, and p-OH-BA

Several preliminary enzymatic tests on commercial samples of the compound of interest were carried out to identify the best reaction conditions (ionic strength and pH values of the buffer) by monitoring the conversion over time through HPLC-DAD. Catalytic oxidation of catechol was studied either in citrate buffer containing 10% of MeOH or directly in unbuffered water. A blank test under the same experimental conditions was also carried out. After 96 h of reaction with the enzyme, an 80.3% conversion was obtained, while conversion was negligible in the blank test (Table 2 and Figure S5). On the other hand, complete conversion of C was obtained in a medium constituted of only unbuffered water. With increasing conversion of C, the progressive formation of a dark precipitate in the reaction mixture was observed. Similar results have been ascribed by other authors to the formation of oxidized oligomeric species (Figure 4) [48–51].

The enzymatic reactions carried out on p-OH-BA and p-OH-AP under the same reaction conditions gave similar results: high conversions, colorless solutions turning dark brown and orange, respectively, within a few hours of reaction, followed by the slow formation of a finely dispersed precipitate. Given the common phenolic structure of C, p-OH-BA and p-OH-AP, it is reasonable to assume that the products obtained from these substrates include oligomeric species, as exemplified for p-OH-BA in Figure 4.

Table 2. Catechol C conversions over time in the enzymatic test and blank experiments in citrate buffer containing 10% methanol.

Reaction Time (h)	C Conversion %	
	Enzymatic Test	Blank
0	0	0
24	30.5	5.5
48	42.2	6.1
72	66.8	7.0
96	80.3	7.5

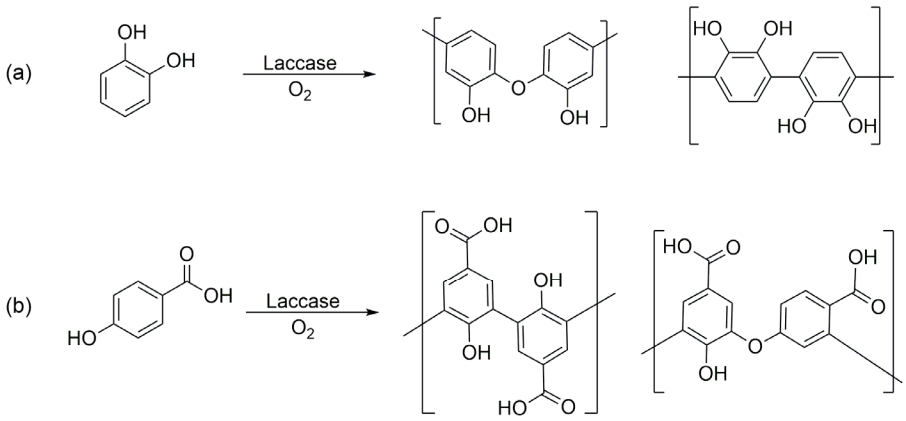


Figure 4. Possible oligomeric products from oxidative oligomerization of C (**a**) and p-OH-BA (**b**).

3.2.2. Enzymatic Reaction on a Mixture of C, p-OH-BA, and p-OH-AP

The enzymatic test was also performed on a mixture of commercial samples of C, p-OH-BA and p-OH-AP to evaluate possible inhibitory and/or competitive effects. The experiment was carried out in unbuffered deionized water to confirm the stability and activity of the enzyme under conditions that more realistically simulated the environmental conditions in which the enzyme typically operates.

The HPLC chromatograms reported in Figure 5 show the individual peaks and their intensity variations over the reaction time, while the conversions over time for each substrate, calculated from the corresponding calibration curve, are reported in Table 3. As is evident from these data, no interference or inhibitory effects on the laccase activity were observed under the adopted conditions. The higher conversion of C may be due to its higher affinity with laccase compared to the two substrates with a carboxyl/carbonyl unit [26]. As observed in the experiments with single compounds, the progressive formation of a dark-brown insoluble residue was observed at high substrate conversions.

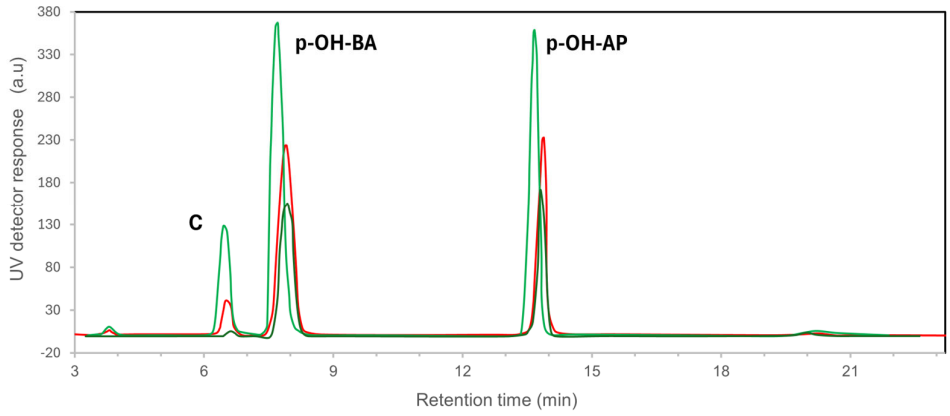


Figure 5. HPLC chromatograms (280 nm) of the enzymatic test on a mixture of C, p-OH-AP, and p-OH-BA at different reaction times (t = 0 light green line, t = 24 h red line, t = 48 h dark green line).

Table 3. Enzymatic test on a mixture of C, p-OH-AP, and p-OH-BA at different reaction times.

Reaction Time (h)	Conversion %		
	C	p-OH-BA	p-OH-AP
0	0	0	0
24	73.1	0	0
48	90.5	32.5	27.4
72	100	53.5	53.3
96	100	77.0	78.0

3.2.3. Enzymatic Reactions on the Extractable from PS_d-UV-5h

Once established that the laccase activity is not significantly affected in unbuffered aqueous medium and in the presence of multiple substrates, enzymatic tests were also carried out on the extracts obtained from PS_d-UV-5h.

Enzymatic Reaction on the Methanol Extract PS_d-UV-MeOH

The methanol extract PS_d-UV-MeOH was dried under reduced pressure (under conditions that do not remove the substrates of interest by volatilization) and then redissolved in the volume of MeOH required to perform the enzymatic test in a 10% v/v methanol/water mixture. The resulting methanolic solution, containing 20 mg of resuspended extract, was added to a laccase solution (1 mL, 40 mg/mL) in citrate buffer (100 mM, pH = 5), giving a final volume of 2.0 mL. The mixture was then allowed to react at 30 °C for 24 h. A blank reaction without enzymes was carried out in parallel. Aliquots of 50 µL of the reaction mixture were withdrawn at regular intervals and analyzed by HPLC-DAD at 254 nm to monitor the progress of the enzymatic reaction. Additional analyses were performed by UPLC-MS-DAD on the initial (t = 0 h) and the final (t = 72 h) reaction mixtures. Chromatographic peaks corresponding to C, p-OH-BA, p-OH-AP and BA were identified by comparison with commercial reference compounds. Peak areas recorded at 280 nm were used for quantitative analysis (Table 4).

Table 4. Enzymatic conversions of C, p-OH-BA, and p-OH-AP contained in the methanol extract PS_d-UV-MeOH (UV at 280 nm).

Compound	Conversion %			
	0 h	**24 h**	**48 h**	**72 h**
C	0	97	100	100
p-OH-BA	0	78.7	100	100
p-OH-AP	0	36.7	36.7	77.9
BA	0	27.8	22.9	26.2

Except for BA (a non-phenolic substrate), all three hydroxylated components were effectively converted by the enzyme. While C and p-OH-BA were completely converted after 48 h, conversion of p-OH-AP progressed at a slower rate up to about 78% after 72 h (Table 4), in general agreement with the results of the enzymatic test carried out on the mixture of the three commercial pure compounds (Table 3) [26].

The UPLC-MS-DAD analysis carried out at the end of the enzymatic reaction (72 h) showed a substantial reduction in the number of sharp peaks compared to the same analysis carried out at the beginning of the test (Figure 6). These results are indicative of the laccase-catalyzed conversion of most of the aromatic compounds generated upon UV degradation of PS into only a few molecular products (sharp chromatographic peaks).

Among the new peaks, the most intense by far had a M/z value corresponding to the BA dimer (peak at 4.67 min r.t.), whereas the BA peak disappeared (Figure 6b), and the very broad signals with maxima at low (r.t. at about 2.90 and 3.50 min) and high (r.t. at about 6 min) retention times suggest the presence of a broad range of higher-molecular-weight oligomeric species.

As in the enzymatic tests with the commercial pure compounds, the PS_d-UV-MeOH mixture also turned into a dark colloidal suspension during the enzymatic reaction, eventually yielding a precipitate that was isolated and characterized by FT-IR and ^{1}H-NMR.

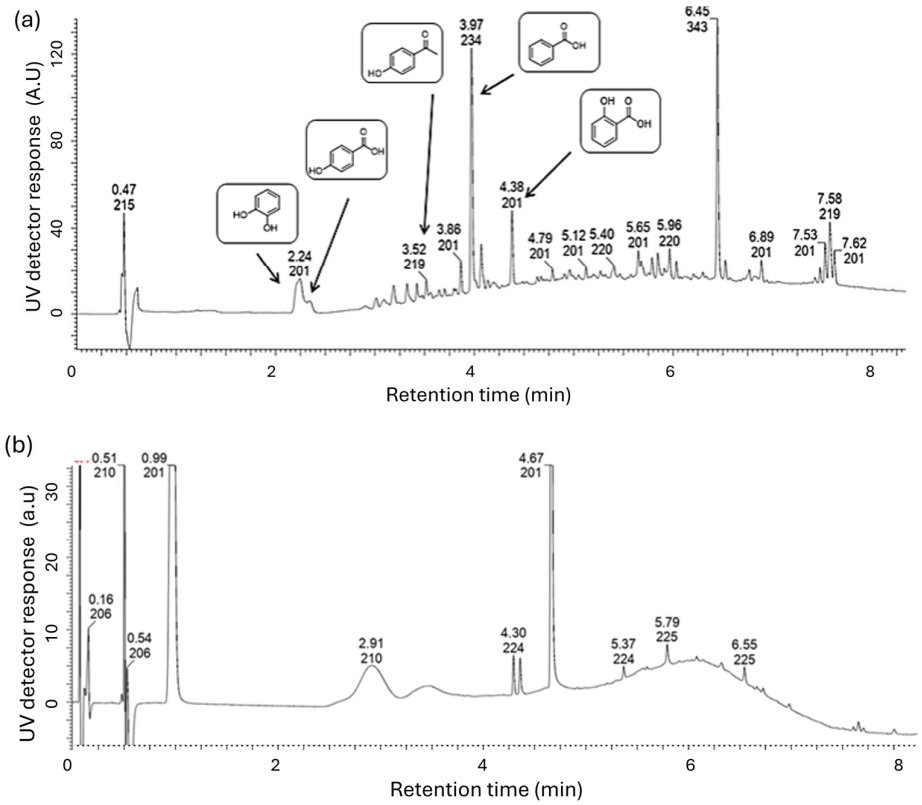


Figure 6. UPLC-MS-DAD chromatogram of the PS_d-UV-MeOH extract before (**a**) and after (**b**) 72 h incubation with the enzyme in a 10:90 MeOH:H_2O mixture. The upper number is the retention time; the lower is the M/z value of the corresponding analyte.

Enzymatic Reaction on the Aqueous Phase of PS_w-UV-5h

The enzymatic reaction also was performed by adding laccase directly to the aqueous phase in which photooxidation of the PS MPs had taken place. These conditions more closely simulate those commonly found in humid environments where microorganisms are more likely to thrive. A total of 500 µL of the aqueous phase was added to 500 µL of a 14 mg/mL solution of laccase and the enzymatic reaction was then performed at T = 30 °C and 600 rpm up to 72 h. Then, 50 µL samples were withdrawn every 24 h and analyzed by HPLC-DAD at 280 nm (Figure S6). Under these conditions, similar enzymatic reaction rates were recorded for the phenolic compounds under study that reached complete conversion after 72 h (Table 5). Lower conversion was observed for benzoic acid.

Table 5. Conversion over time of C, p-OH-BA, p-OH-AP and BA in the aqueous phase of PS_w-UV-5h.

Compound	Conversion %			
	0 h	**24 h**	**48 h**	**72 h**
C	0	24.5	100	100
p-OH-BA	0	18.9	100	100
p-OH-AP	0	21.0	95.6	98.2
BA	0	0	21.8	39.0

A progressive darkening of the reacting mixtures (initially transparent and then cloudy due to the formation of a colloidal suspension) was observed as in the previous experiment performed on the PS_d-UV-MeOH extract (see Section 3.2.3).

Enzymatic Activity Determination Assays of Laccase

The enzymatic activity under the standard assay conditions was evaluated in the presence or absence of the methanol extract of PS_d-UV-5h. The determination of laccase activity is usually performed by spectrophotometric monitoring of the increase in absorbance caused by the oxidation of methoxyphenols such as syringaldazine, used here as a standard substrate, compared to the corresponding quinone [36]. The study showed that the number of enzymatic activity units of laccase over time is higher in the presence of the methanol extract of PS_d-UV-5h than in the blank test (Table S4). This can be explained by possible stabilizing effects on the catalytically active conformation of the enzyme promoted by the aromatic compounds, preventing the partial/slow denaturation occurring in purely aqueous solution.

3.3. Characterization of the Precipitates Isolated from Laccase-Catalyzed Reactions

The insoluble dark-brown precipitate from laccase-catalyzed reactions on C was isolated by filtration and characterized by FT-IR spectroscopy. By inspection of the two spectra in Figure 7, the product of the enzymatic reaction of C presents significant differences from its precursor: (i) a broader and featureless strong absorption peaking at about 3500 cm^{-1} (C-C vibrations), replacing the previous two main peaks in the alcoholic and carboxylic O-H stretching region (3500–3300 cm^{-1}); (ii) the aromatic C-H stretching peaks (3050–3000 cm^{-1}) become more prevalent with respect to the aliphatic equivalent (2960–2850 cm^{-1}); (iii) significant changes occur in the aromatic C-C vibration region (1400–1600 cm^{-1}), with a broad vibrational band at around 1611 cm^{-1} ascribed to the ortho-bis-substituted benzene ring stretching, possibly from condensed ring structures; (iv) in the region including various C-O-C stretching modes (1280–1000 cm^{-1}), with new notable phenyl ether asymmetric and symmetric stretching absorptions at 1270 cm^{-1} and 1030 cm^{-1}, respectively [49]; (v) in the region of the aromatic C-H deformations (950–700 cm^{-1}), with two notable new peaks at 820 and 700 cm^{-1} (likely due to out-of-plane C-H deformation from aromatic fused rings).

The aromatic region of the ^{1}H-NMR spectrum recorded from the precipitate isolated from the laccase reaction on C revealed an increased complexity of the aromatic protons, in agreement with the possible conversion into oligomeric and/or condensed polycyclic aromatic structures.

The results of the spectroscopic characterization of the brown precipitates obtained after laccase reaction on p-OH-BA and p-OH-AP gave similar indications as those discussed above for C.

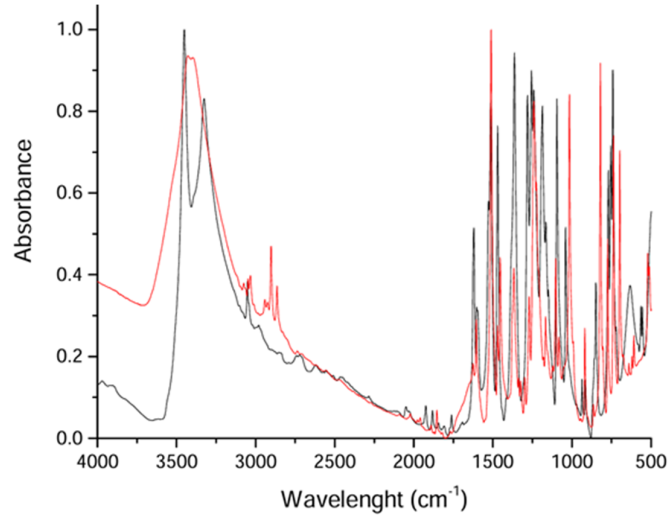
The ^{1}H-NMR spectra of the precipitate from p-OH-BA enzymatic reaction (Figure S7 in the SI) presents an increased number of aromatic proton resonances as compared to the precursor substrate, as one would expect from the formation of oligomeric aromatic structures [30]. Similar results were observed by comparing the ^{1}H-NMR spectra of p-OH-AP and the precipitate from its laccase reaction (Figure S8). In particular, the spectrum of the precipitate showed an increased complexity in the aromatic zone and new resonances at 5.25 ppm attributable to different types of alpha-carbonyl protons.

These signals, which could be assigned to diaryl ether (6.5–8.0 ppm) or alkylaryl ether bridges among aromatic moieties (4.5, 6.5–8.0 ppm), aromatic C-C bonds (8.0 ppm) and ketoaromatic groups (6.5–8.0 ppm), suggested the formation of oligomeric structures such as those hypothesized in Figure 8 [31].

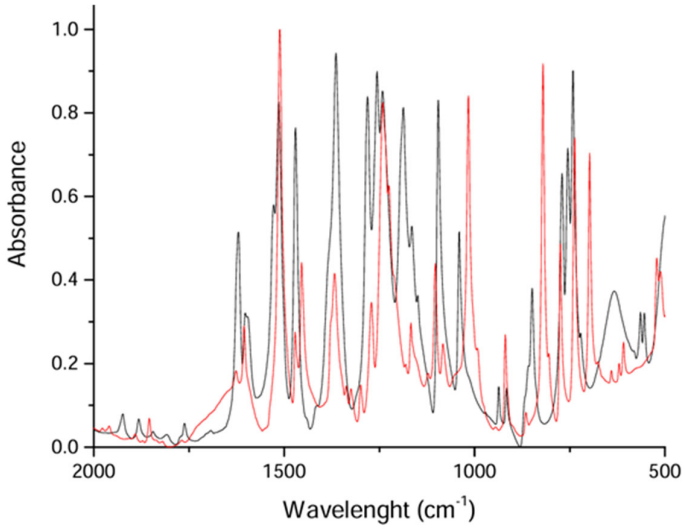
Additional absorptions in the FT-IR spectra of the brown precipitate from p-OH-BA (Figure S9 in the SI) and of the orange precipitate from p-OH-AP (Figure S10 in the SI) suggest the presence of different types of keto groups in the precipitate from p-OH-AP (broad carbonyl absorption) and the presence of diaryl C-C, diaryl ether and alkylaryl

ether bonds (1300–1210 cm^{-1}) forming the junctions between aromatic units in oligomeric structures such as those reported in Figures 4 and 8.

To further confirm the conversion of the reference phenolic compounds into oligomeric products, the precipitate obtained under experimental conditions analogous to those described in Section 3.2.2 was collected and dried under vacuum to constant weight (Table 6).



(**a**)



(**b**)

Figure 7. FTIR spectra of C (black line) and of the high-molecular-weight (polymeric) product precipitated after its enzymatic conversion (red line): (**a**) whole spectrum; (**b**) diagnostic absorption region for oxidized aromatic groups: 1280–1000 cm^{-1} C-O-C stretching and 1270 and 1030 cm^{-1} phenyl ether asymmetric and symmetric stretching.

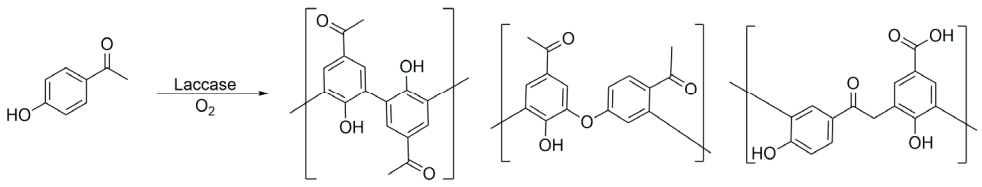


Figure 8. Possible structures deriving from the polymerization of p-O-AP.

Table 6. Yields of precipitated products from the laccase oxidation of C, p-OH-BA, p-OH-AP, and their mixture.

Compound	(mg)	Precipitated Residue (mg)	Yield (%)
C	10.0	7.6	76.0
p-OH-BA	10.3	1.9	18.4
p-OH-AP	9.8	4.3	43.9
Mixture [a]	30.1	11.2	37.2

[a] The mixture was obtained by mixing 10 mg each of the three compounds.

Molecular weight analysis of the obtained precipitates was performed by GPC with UV detection at 260 and 370 nm (Figure S11). The calculations performed on the two main chromatographic fractions of the polymodal distribution (number- and weight-average molecular weights relative to polystyrene calibration are reported in Table 7) confirmed that the molecular weights of the precipitated products from the laccase enzymatic reaction were higher than those of the corresponding substrate, confirming that laccase can catalyze condensation and possibly oligomerization of water-soluble phenolic products of photooxidative degradation of PS.

Table 7. GPC data of precipitated products from enzymatic reaction on C, p-OH-BA, p-OH-AP and BA.

Compound	1° Peak			2° Peak		
	$\overline{M}_n$ [Da]	$\overline{M}_w$ [Da]	PDI	$\overline{M}_n$ [Da]	$\overline{M}_w$ [Da]	PDI
C	819	844	1.03	563	565	1.003
p-OH-BA	702	765	1.09	277	278	1.005
p-OH-AP	766	777	1.01	558	560	1.004
BA	1006	1183	1.18	562	565	1.005

4. Conclusions

A large number of low-molecular-weight compounds (up to approximately 350 g/mol) with different polarities (HyPOPs) were identified in the aqueous leachate from photooxidized PS. The most abundant species were C, p-OH-AP, p-OH-BA and BA, along with smaller amounts of aliphatic compounds originating from the homolytic cleavage of the C-C bonds between the pendant phenyl moieties rings and the aliphatic main chain of PS. A slightly larger amount of extractables, including oligomeric fragments (up to 700 g/mol), was obtained in methanolic leachates. The ligninolytic oxidase laccase from *Trametes versicolor*, tested on the four HyPOPs listed above as reference substrates, led to the formation of new metabolites and of significant amounts of high-molecular-weight humic acid analogs. In addition, the presence of the substrate positively influenced the enzyme activity, likely as the result of the enzyme–substrate interaction stabilizing the transition state and/or the most catalytically active enzyme conformation.

The present investigation extends beyond previous studies, in which laccase has mainly been evaluated as a key agent in the biotransformation of lignocellulosic biomass into humic acids. Our results highlight the potential of enzymatic systems naturally occurring in soil as key players in the biotransformation and re-organication of potentially toxic xenobiotic substances, such as those deriving from the environmental degradation of PS. This is particularly relevant when macroscopic plastic debris is progressively degraded into micro- and nanoplastics, which are characterized by much higher specific surface areas and therefore more intensive environmental exposure and faster degradation rates. Besides removing the toxic PS degradation products, the laccase-catalyzed production of humic acid

analogs, capable of sequestering heavy metals and storing water and nutrients, highlights the potentially significant role of fungal laccases in turning a source of contamination into a natural route to improved soil quality. Finally, the versatile approach discussed in the present work, consisting of the assessment of the enzymatic transformations of molecular degradation products deriving from photooxidized PS MPs, may be extended to other polymeric materials also capable of generating MPs and the associated leachable degradation products upon environmental aging.

Supplementary Materials: The following supporting information can be downloaded at https://www.mdpi.com/article/10.3390/microplastics5010041/s1. Table S1: Chromatographic peak area used for the linear fit calibration of C; Table S2: Chromatographic peak area used for the linear fit calibration of p-OH-BA and p-OH-AP; Table S3: Main products identified through GC-MS of PS_d-UV-5h water extract; Table S4: Enzymatic activity of laccase in the presence of PS_d-UV-5h methanol extract. Figure S1: Linear fit for the chromatographic calibration of C concentration; Figure S2: Linear fit for the chromatographic calibration of p-OH-BA concentration; Figure S3: Linear fit for the chromatographic calibration of p-OH-AP concentration; Figure S4: Linear fit for the chromatographic calibration of BA concentration; Figure S5: HPLC chromatograms performed at different reaction times using catechol as reference substrate; Figure S6: HPLC chromatograms of samples from the enzymatic test on aqueous phases at different reaction times; Figure S7: 1H-NMR spectrum ($CDCl_3$ at 400 MHz) of the enzymatic degradation products of p-OH-BA; Figure S8: FTIR spectra of p-OH-BA and of the high-molecular-weight (polymeric) product obtained by its enzymatic conversion; Figure S9: FTIR spectra of p-OH-AP and of the high-molecular-weight (polymeric) product obtained from its enzymatic conversion; Figure S10: GPC chromatogram of p-OH-acetophenone enzymatic degradation products; Figure S11: GPC chromatogram of p-OH-acetophenone enzymatic degradation products.

Author Contributions: Conceptualization, A.C., A.P. and M.L.; methodology, A.C., A.P. and V.C.; validation, D.A., A.C. and A.P.; investigation, F.P. and D.A.; resources, A.P. and V.C.; data curation, F.P. and D.A.; writing—original draft preparation, F.P. and D.A.; writing—review and editing, A.C., A.P. and V.C.; supervision, A.P.; funding acquisition, V.C. and A.P. All authors have read and agreed to the published version of the manuscript.

Funding: This research was supported by the National Key R&D Program of China (2023YFE0117000), the Italian Ministry of Foreign Affairs and International Cooperation (grant PGR02013, ENCOMPASS project) and the University of Pisa (PRA_2020_27).

Data Availability Statement: The raw data supporting the conclusions of this article will be made available by the authors on request.

Acknowledgments: The authors thank Stefania Giannarelli for kindly providing the preliminary GC-MS analysis of PS-UV extracts.

Conflicts of Interest: The authors declare no conflicts of interest.

Abbreviations

The following abbreviations are used in this manuscript:

AP	acetophenone
BA	benzoic acid
C	catechol
HyPOPs	hydrophilic photooxidation products
MNPs	micro and nanoplastics
MPs	microplastics
NPs	nanoplastics
p-OH-AP	para-hydroxyacetophenone
o-OH-BA	ortho-hydroxybenzoic acid
p-OH-BA	para-hydroxybenzoic acid

PDI	polydispersity index
PE	polyethylene
PET	polyethylene terephthalate
PP	polypropylene
PS	polystyrene
PS_d-UV	product of UV aging of PS as a dry micropowder
PS_w-UV	product of UV aging of PS micropowder in water
PS_d-UV-MeOH	fraction of PS_d-UV extractable in methanol
SET	single-electron transfer

References

1. Thakur, S.; Verma, A.; Sharma, B.; Chaudhary, J.; Tamulevicius, S.; Thakur, V.K. Recent developments in recycling of polystyrene-based plastics. *Curr. Opin. Green Sustain. Chem.* **2018**, *13*, 32–38. [CrossRef]
2. Geyer, R.; Jambeck, J.R.; Law, K.L. Production, use, and fate of all plastics ever made. *Sci. Adv.* **2017**, *3*, e1700782. [CrossRef] [PubMed]
3. Van Cauwenberghe, L.; Janssen, C.R. Microplastics in bivalves cultured for human consumption. *Environ. Pollut.* **2014**, *193*, 65–70. [CrossRef] [PubMed]
4. Nelms, S.E.; Barnett, J.; Brownlow, A.; Davison, N.J.; Deaville, R.; Galloway, T.S.; Lindeque, P.K.; Santillo, D.; Godley, B.J. Microplastics in marine mammals stranded around the British coast: Ubiquitous but transitory? *Sci. Rep.* **2019**, *9*, 1075. [CrossRef]
5. Kosuth, M.; Mason, S.A.; Wattenberg, E.V. Anthropogenic contamination of tap water, beer, and sea salt. *PLoS ONE* **2018**, *13*, e0194970. [CrossRef]
6. Hwang, J.; Choi, D.; Han, S.; Jung, S.Y.; Choi, J.; Hong, J. Potential toxicity of polystyrene microplastic particles. *Sci. Rep.* **2020**, *10*, 7391. [CrossRef]
7. Leibman, K.C. Metabolism and toxicity of styrene. *Environ. Health Perspect.* **1975**, *11*, 115–119. [CrossRef]
8. Bond, J.A.; Bolt, H.M. Review of the toxicology of styrene. *CRC Crit. Rev. Toxicol.* **1989**, *19*, 227–249. [CrossRef]
9. Solomon, G.M.; Weiss, P.M. Chemical contaminants in breast milk: Time trends and regional variability. *Environ. Health Perspect.* **2002**, *110*, A339–A347. [CrossRef]
10. Ramamurthy, K.; Thomas, N.P.; Gopi, S.; Sudhakaran, G.; Haridevamuthu, B.; Namasivayam, K.R.; Arockiaraj, J. Is laccase derived from *Pleurotus ostreatus* effective in microplastic degradation? A critical review of current progress, challenges, and future prospects. *Int. J. Biol. Macromol.* **2024**, *276*, 133971. [CrossRef]
11. Kim, Y.-B.; Kim, S.; Park, C.; Yeom, S.-J. Biodegradation of polystyrene and systems biology-based approaches to the development of new biocatalysts for plastic degradation. *Curr. Opin. Sys. Biol.* **2024**, *37*, 100505. [CrossRef]
12. Singh, P.; Lau, C.S.S.; Siah, S.Y.; Chua, K.O.; Ting, A.S.Y. Microbial degradation of low-density polyethylene, polyethylene terephthalate, and polystyrene by novel isolates from plastic polluted environment. *Arch. Microbiol.* **2024**, *206*, 188. [CrossRef]
13. Zhang, J.; Shao, Y.; Shao, Y.; Yang, W.; Xuan, N.; Geng, Y.; Bian, F.; Zhang, Y.; Chen, G. Pretreated polystyrene is degraded by a microbial consortium enriched from wetland plastic waste. *J. Hazard. Mater.* **2024**, *480*, 136143. [CrossRef] [PubMed]
14. Mor, R.; Sivan, A. Biofilm formation and partial biodegradation of polystyrene by the actinomycete *Rhodococcus ruber*: Biodegradation of polystyrene. *Biodegradation* **2008**, *19*, 851–858. [CrossRef] [PubMed]
15. Castelvetro, V.; Corti, A.; Biale, G.; Ceccarini, A.; Degano, I.; La Nasa, J.; Lomonaco, T.; Manariti, A.; Manco, E.; Modugno, F.; et al. New methodologies for the detection, identification, and quantification of microplastics and their environmental degradation by-products. *Environ. Sci. Pollut. Res.* **2021**, *28*, 46764–46780. [CrossRef]
16. Lomonaco, T.; Manco, E.; Corti, A.; La Nasa, J.; Ghimenti, S.; Biagini, D.; Di Francesco, F.; Modugno, F.; Ceccarini, A.; Fuoco, R.; et al. Release of harmful volatile organic compounds (VOCs) from photo-degraded plastic debris: A neglected source of environmental pollution. *J. Hazard. Mater.* **2020**, *394*, 122596. [CrossRef]
17. Ho, B.T.; Roberts, T.K.; Lucas, S. An overview on biodegradation of polystyrene and modified polystyrene: The microbial approach. *Crit. Rev. Biotechnol.* **2018**, *38*, 308–320. [CrossRef]
18. Heim, K.E.; Tagliaferro, A.R.; Bobilya, D.J. Flavonoid antioxidants: Chemistry, metabolism and structure-activity relationships. *J. Nutr. Biochem.* **2002**, *13*, 572–584. [CrossRef]
19. Lee, S.; Alam, M.B.; Jung, M.J.; Lee, S.; Liu, K.H.; Lee, S.H.; Kim, S. Identification and Toxicity Evaluation of Water-Soluble Chemicals Generated by the Photooxidative Degradation of Expanded Polystyrene. *Front. Environ. Sci.* **2022**, *10*, 938120. [CrossRef]
20. Mills, W.B.; Porcella, D.B.; Ungs, M.J.; Gherini, S.A.; Summers, K.V.; Mok, L.; Rupp, G.L.; Bowie, G.L.; Haith, D.A. *Water Quality Assessment: A Screening Procedure for Toxic and Conventional Pollutants in Surface and Ground Water*; Report EPA/600/6-85/002; Environmental Research Laboratory, Office of Research and Development, US Environmental Protection Agency: Washington, DC, USA, 1985.

21. Oikawa, S.; Hirosawa, I.; Hirakawa, K.; Kawanishi, S. Site specificity and mechanism of oxidative DNA damage induced by carcinogenic catechol. *Carcinogenesis* **2001**, *22*, 1239–1245. [CrossRef]
22. Krogmeier, M.J.; Bremner, J.M. Effects of phenolic acids on seed germination and seedling growth in soil. *Biol. Fertil. Soils* **1989**, *8*, 116–122. [CrossRef]
23. Gonzalez, M.D.; Moreno, E.; Quevedo-Sarmiento, J.; Ramos-Cormenzana, A. Studies on antibacterial activity of waste waters from olive oil mills (alpechin): Inhibitory activity of phenolic and fatty acids. *Chemosphere* **1990**, *20*, 423–432. [CrossRef]
24. Maisto, M.; Zuzolo, D.; Tartaglia, M.; Prigioniero, A.; Ranauda, M.A.; Germinario, C.; Falzarano, A.; Castelvetro, V.; Sciarrillo, R.; Guarino, C. Advances in plastic mycoremediation: Focus on the isoenzymes of the lignin degradation complex. *Sci. Total Environ.* **2024**, *948*, 17455. [CrossRef] [PubMed]
25. Thurston, C.F. The structure and function of fungal laccases. *Microbiology* **1994**, *140*, 19–26. [CrossRef]
26. Reinhammar, B.; Malmström, B.G. Blue copper-containing oxidases. In *Copper Proteins Copper Enzymes*; Spiro, T.G., Ed.; Wiley-Interscience: New York, NY, USA, 1981; pp. 1–35.
27. Canfora, L.; Iamarino, G.; Rao, M.A.; Gianfreda, L. Oxidative transformation of natural and synthetic phenolic mixtures by *Trametes versicolor* laccase. *J. Agric. Food Chem.* **2008**, *56*, 1398–1407. [CrossRef]
28. Sharma, K.K.; Kuhad, R.C. Laccase: Enzyme revisited and function redefined. *Indian J. Microbiol.* **2008**, *48*, 309–316. [CrossRef]
29. Gianfreda, L.; Bollag, J.M. Isolated enzymes for the transformation and detoxification of organic pollutants. In *Enzymes in the Environment: Activity, Ecology, and Applications*; Burns, R.G., Dick, R.P., Eds.; Marcel Dekker: New York, NY, USA, 2002; pp. 495–538.
30. Slagman, S.; Escorihuela, J.; Zuilhof, H.; Franssen, M.C. Characterization of the laccase-mediated oligomerization of 4-hydroxybenzoic acid. *RSC Adv.* **2016**, *6*, 99367–99375. [CrossRef]
31. Grosso, S.; Radaelli, F.; Fronza, G.; Passarella, D.; Monti, D.; Riva, S. Studies on the Laccase-Catalyzed Oxidation of 4-Hydroxy-Chalcones. *Adv. Synth. Catal.* **2019**, *361*, 2696–2705. [CrossRef]
32. Panagiotis, E.A.; Gkountela, C.I.; Patila, M.; Fotiadou, R.; Chatzikonstantinou, A.V.; Vouyiouka, S.N.; Stamatis, H. Laccase-mediated oxidation of phenolic compounds from wine lees extract towards the synthesis of polymers with potential applications in food packaging. *Biomolecules* **2024**, *14*, 323. [CrossRef]
33. Dec, J.; Bollag, J.M. Phenoloxidase-mediated interactions of phenols and anilines with humic materials. *J. Environ. Qual.* **2000**, *29*, 665–676. [CrossRef]
34. Witayakran, S.; Ragauskas, A.J. Synthetic applications of laccase in green chemistry. *Adv. Synth. Catal.* **2009**, *351*, 1187–1209. [CrossRef]
35. De Melo, B.A.G.; Motta, F.L.; Santana, M.H.A. Humic acids: Structural properties and multiple functionalities for novel technological developments. *Mater. Sci. Eng. C* **2016**, *62*, 967–974. [CrossRef] [PubMed]
36. Manole, A.; Herea, D.; Chiriac, H.; Melnig, V. Laccase activity determination. *Biomater. Biophys. Med. Phys. Ecol.* **2008**, *1*, 1–8.
37. Tian, L.; Chen, Q.; Jiang, W.; Wang, L.; Xie, H.; Kalogerakis, N.; Ma, Y.; Ji, R. A carbon-14 radiotracer-based study on the photo transformation of polystyrene nanoplastics in water versus in air. *Environ. Sci. Nano* **2019**, *6*, 2907–2917. [CrossRef]
38. Ranby, B.; Lucki, J. New aspects of photodegradation and photooxidation of polystyrene. *Pure Appl. Chem.* **1980**, *52*, 295–303. [CrossRef]
39. Yousif, E.; Haddad, R. Photodegradation and photostabilization of polymers, especially polystyrene. *SpringerPlus* **2013**, *2*, 398. [CrossRef]
40. Gardette, J.L.; Mailhot, B.; Lemaire, J. Photooxidation mechanisms of styrenic polymers. *Polym. Degrad. Stab.* **1995**, *48*, 457–470. [CrossRef]
41. Lee, S.; Kim, S. Study on Photodegradable Water-Soluble Compounds of Expanded Polystyrene. *Mass Spectrom. Lett.* **2021**, *12*, 118–124.
42. Du, Y.; Yao, C.; Dou, M.; Wu, J.; Su, L.; Xia, W. Oxidative degradation of pre-oxidated polystyrene plastics by dye decolorizing peroxidases from *Thermomonospora curvata* and *Nostocaceae*. *J. Hazard. Mater.* **2022**, *436*, 129265. [CrossRef]
43. Tsochatzis, E.D.; Berggreen, I.E.; Nørgaard, J.V.; Theodoridis, G.; Dalsgaard, T.K. Biodegradation of expanded polystyrene by mealworm larvae under different feeding strategies evaluated by metabolic profiling using GC-TOF-MS. *Chemosphere* **2021**, *281*, 130840. [CrossRef]
44. Li, C.; Jiang, B.; Guo, J.; Sun, C.; Shi, C.; Huang, S.; Liu, W.; Wu, C.; Zhang, Y. Aging process of microplastics in the aquatic environments: Aging pathway, characteristic change, compound effect, and environmentally persistent free radicals' formation. *Water* **2022**, *14*, 3515. [CrossRef]
45. Biale, G.; La Nasa, J.; Mattonai, M.; Corti, A.; Vinciguerra, V.; Castelvetro, V.; Modugno, F. A systematic study on the degradation products generated from artificially aged microplastics. *Polymers* **2021**, *13*, 1997. [CrossRef] [PubMed]
46. Fabbri, D.; Carena, L.; Bertone, D.; Brigante, M.; Passananti, M.; Vione, D. Assessing the photodegradation potential of compounds derived from the photoinduced weathering of polystyrene in water. *Sci. Total Environ.* **2023**, *876*, 162729. [CrossRef]

47. Liu, X.; Sun, P.; Qu, G.; Jing, J.; Zhang, T.; Shi, H.; Zhao, Y. Insight into the characteristics and sorption behaviors of aged polystyrene microplastics through three type of accelerated oxidation processes. *J. Hazard. Mater.* **2021**, *407*, 124836. [CrossRef]
48. Ahn, M.Y.; Martínez, C.E.; Archibald, D.D.; Zimmerman, A.R.; Bollag, J.M.; Dec, J. Transformation of catechol in the presence of a laccase and birnessite. *Soil Biol. Biochem.* **2006**, *38*, 1015–1020. [CrossRef]
49. Aktaş, N.; Tanyolaç, A. Reaction conditions for laccase catalyzed polymerization of catechol. *Bioresour. Technol.* **2003**, *87*, 209–214. [CrossRef]
50. Avci, G.K.; Ogel, Z.B. Oxidation of catechol, (+)-catechin, and caffeic acid by the laccase from *Trametes versicolor* and tyrosinase from *Agaricus bisporus*. *J. Turk. Vet. Med. Soc.* **2014**, *85*, 20–34.
51. Dubey, S.; Singh, D.; Misra, R.A. Enzymatic synthesis and various properties of poly (catechol). *Enzym. Microb. Technol.* **1998**, *23*, 432–437. [CrossRef]

Disclaimer/Publisher's Note: The statements, opinions and data contained in all publications are solely those of the individual author(s) and contributor(s) and not of MDPI and/or the editor(s). MDPI and/or the editor(s) disclaim responsibility for any injury to people or property resulting from any ideas, methods, instructions or products referred to in the content.